Chapter 11
Zoonotic Disease, Avian Influenza, and Nonautonomous Models

11.1 Introduction

Zoonotic diseases are contagious diseases that are transmitted between animals and humans. These diseases are caused by bacteria, viruses, parasites, fungi, and prions that are carried by animals and insects.

Zoonotic diseases include vector-borne diseases but also diseases transmitted by vertebrate animals. For some zoonotic diseases, humans are a host that can pass on the pathogen to the animals or to the environment, while for others, the humans are a dead-end host. Examples of the first type are cholera, ebola, and malaria. Examples of the second kind are Rift Valley fever, hantavirus, West Nile virus, and avian influenza.

Zoonotic diseases play a very important role among human communicable diseases. In a review of more than 1400 pathogens known to infect humans, it was found that more than 61% were zoonotic [149]. Zoonotic diseases often serve as a starting point of many pathogens that jump the species barrier and become effectively human-to-human transmissible. Such diseases are called *emergent diseases*.

One of the most dangerous zoonotic pathogens is avian influenza H5N1. Avian influenza is transmitted from birds to humans. As of May 2014, H5N1 has infected more of 600 humans, 60% of whom have died. Besides the high mortality, what makes H5N1 dangerous is the possibility for the pathogen to mutate or reassort into a highly human-to-human transmissible flu pathogen with high mortality. In such a case, a world pandemic would occur, but since humans have no prior exposure to the H5 subtype of influenza A, mortality may be higher than it was in the 2009 H1N1 pandemic, caused by the "swine flu."

M. Martcheva, *An Introduction to Mathematical Epidemiology*,
Texts in Applied Mathematics 61, DOI 10.1007/978-1-4899-7612-3_11

11.2 Modeling Avian Influenza

Modeling zoonotic diseases in general, and avian influenza in particular, involves modeling transmission in several species. Many of the zoonotic diseases involve multiple species. For instance, the avian influenza pathogen infects wild birds, domestic birds, humans, and many animal species such as pigs and cats. One has to decide which species are important to the transmission.

In the case of avian influenza, we typically want to address questions related to human health. Humans are a dead-end host for H5N1, but H5N1 transmits to humans from domestic birds. It transmits effectively in birds and is endemic in the poultry populations in some countries.

11.2.1 Simple Bird–Human Avian Influenza Model

One of the simplest models of avian influenza (AI) was proposed by Iwami [80], following whom, we model transmission in poultry and the spillover to humans. H5N1 is very deadly for chickens. Mortality reaches 90–100% typically within 48 h [40]. This suggests that a simple SI model with disease-induced mortality is a good tool to model the transmission within poultry.

$$\textbf{Domestic Birds:} \begin{cases} S_d'(t) = \Lambda_d - \beta_d S_d I_d - \mu_d S_d, \\ I_d'(t) = \beta_d S_d I_d - (\mu_d + \nu_d) I_d, \end{cases} \tag{11.1}$$

where S_d is the number of susceptible birds, I_d is the number of infected birds, Λ_d is the recruitment rate, μ_d is the poultry natural death rate, ν_d is the disease-induced death rate, and β_d is the transmission coefficient among poultry. Humans become infected from touching infected uncooked poultry products. The spillover model for humans takes the form

$$\textbf{Humans:} \begin{cases} S'(t) = \Lambda - \beta S I_d - \mu S, \\ I'(t) = \beta S I_d - (\mu + \nu) I, \end{cases} \tag{11.2}$$

where S is the number of susceptible humans, I is the number of infected humans, Λ is the recruitment rate for humans, μ is the human natural death rate, ν is the disease-induced death rate for humans, and β is the transmission coefficient from infected poultry to humans.

The dynamics of the solutions to model (11.1)–(11.2) are not very different from those of the SI poultry model. The model has a reproduction number

$$\mathscr{R}_d = \frac{\Lambda_d \beta_d}{\mu_d(\mu_d + \nu_d)}.$$

If $\mathscr{R}_d < 1$, then all solutions approach the disease-free equilibrium: $\mathscr{E}_0 = (\frac{\Lambda_d}{\mu_d}, 0, \frac{\Lambda}{\mu}, 0)$. If $\mathscr{R}_d > 1$, then all solutions approach the endemic equilibrium $\mathscr{E}^* = (S_d^*, I_d^*, S^*, I^*)$,

where

$$S_d^* = \frac{\mu_d + \nu_d}{\beta_d}, \qquad I_d^* = \frac{\mu_d}{\beta_d}(\mathscr{R}_d - 1), \qquad S^* = \frac{\Lambda}{\beta I_d^* + \mu} \qquad I^* = \frac{\beta S^* I_d^*}{\mu + \nu}.$$

We see that if $\beta \neq 0$, then the outcome of the disease in humans is a direct consequence of the outcome of the disease in poultry.

11.2.2 Parameterizing the Simple Avian Influenza Model

One of the main ingredients in developing models is determining reasonable parameter values for the model. We fix the time unit in years. The reason for that will become clear later. Determining parameters is typically done through fitting. Model (11.1)–(11.2) has eight parameters and four unknown initial conditions. The main data source is the cumulative number of H5N1 human cases given by the World Health Organization [166]. We give the data in Table 11.1.

Table 11.1 Number of cumulative human cases of H5N1 in units 10^5

Year	Time	Cases	Year	Time	Cases
2005	0	0.00047	2010	5	0.00467
	0.5	0.00108		5.5	0.005
2006	1	0.00148	2011	6	0.00516
	1.5	0.00229		6.5	0.00562
2007	2	0.00263	2012	7	0.00576
	2.5	0.00318		7.5	0.00607
2008	3	0.00351	2013	8	0.00610
	3.5	0.00387		8.5	0.00633
2009	4	0.00395	2014	9	0.0065
	4.5	0.00436			

If the data are taken at half-year intervals, that will give 19 data points, potentially not enough to fit all parameters and initial conditions. A better approach is to predetermine some of the parameters. The Food and Agriculture Organization of the United Nations (FAO) publishes statistics on livestock [58]. FAO gives that in 2012, there were 24 billion units of poultry worldwide [58]. We set the world's poultry population at 2400×10^7. Iwami [81] gives the mean lifespan of poultry to be two years. That translates into $\mu_d = 0.5$. Since the entire population Λ_d/μ_d is equal to 2400 we have $\Lambda_d = 1200$ in units of 10^7 per year. Iwami [81] also uses mean infectious period for domestic birds of 10 days, that is, $\nu_d = 36.5$ years^{-1}.

The natural lifespan of humans throughout the world varies significantly from country to country. We take an average value of human lifespan to be 65 years. Therefore, $\mu = 1/65$. The world human population has been on average approximately 6.5 billion over these 10 years. That gives a value of $\Lambda = 1000$ births per

year in units of 10^5 individuals. Finally, we preestimate some of the initial conditions: $S_d(0) = 2400$, $I(0) = 0.0007$ and $S(0) = 65000$.

Alternatively, one can get the information about the poultry and the human population of only the affected countries, of which there are 16. Data exist in the same data sources. This is left as an exercise (see Problem 11.1).

To determine $\beta_d, \beta, I_d(0)$, we fit the model (11.1)–(11.2) to the data, and we estimate $I_d(0) = 0.3936$, $\beta = 0.000000035327684$, and $\beta_d = 0.015489231377$. The fit is given in Fig. 11.1. The Matlab code that executes the fitting is given in the appendix.

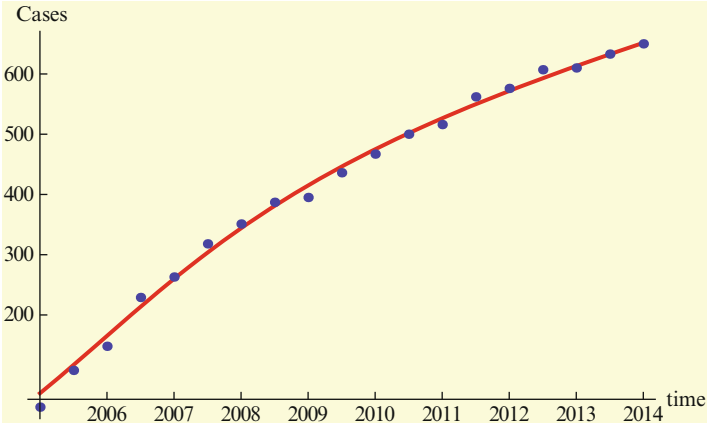

Fig. 11.1 Fit of model (11.1)–(11.2) to cumulative number of human cases of H5N1 given in Table 11.1

The estimated reproduction number with the fitted data is $\mathscr{R}_d = 1.00471$.

11.2.3 Evaluating Avian Influenza Control Strategies

Control strategies that are currently in place have the goal of delaying or preventing the emergence of a pandemic H5N1 strain. These measures currently involve the following [108]:

- Vaccination of poultry;
- Culling/destroying infected and potentially exposed poultry;
- Reducing contact with poultry by wearing protective gear;
- Isolation of humans infected with H5N1 and tracing the source of infection of the isolated individuals;
- Increasing biosecurity of poultry rearing;
- Education of poultry workers and health personnel.

Multiple control measures are applied differently in different countries. Evaluating their overall effectiveness is not a trivial task. Typically, this is done by collecting the opinions of experts. Here we present a more objective approach. Suppose the goal of the control measures is to reduce the number of cases of H5N1 in humans, that is, the goal is to minimize I^*. Each of the control measures impacts certain parameter values. We evaluate the change that a 1% change in a parameter p makes on I^* through the concept of elasticity. Recall that the elasticity of I^* with respect to the parameter p is given by

$$\varepsilon_p = \frac{\partial I^*}{\partial p}\frac{p}{I^*}, \tag{11.3}$$

where

$$I^* = \frac{\Lambda}{\mu+\nu}\frac{\beta\mu_d(\mathscr{R}_d-1)}{\beta\mu_d(\mathscr{R}_d-1)+\mu\beta_d}.$$

We use Mathematica to compute the elasticities with the above-evaluated parameters. The elasticities are listed in Table 11.2.

Table 11.2 Table of elasticities of I^*

Parameter	Elasticity	Parameter	Elasticity
β_d	212.454	β	1
μ_d	−215.338	μ	− 1.00042
ν_d	−210.569	ν	− 0.999579
Λ_d	213.454	Λ	1

From this table, we see directly that control measures that are applied to poultry and affect poultry parameters are much more effective in influencing the prevalence in humans than control measures applied to humans. This result seems robust and independent of the model [108]. To compare the control measures, we determine which parameters each control measure would affect. For instance, culling affects μ_d and ν_d. Culling with repopulation affects μ_d, ν_d, and Λ_d. Vaccination affects β_d and ν_d. Wearing protective gear affects β. We define the overall effect of the control measure to be the sum of efficacies of the effect of the measure on each affected parameter. For instance, culling with repopulation increases Λ_d and increases μ_d and ν_d. Hence, the overall efficacy is $213.454 - 210.569 - 215.338 = -212.453$. We will take this number as an absolute value. We summarize the overall effects of each control measure in Table 11.3. The affected parameters in the educational control measure are hard to pinpoint and are omitted.

Table 11.3 suggests that culling without repopulation is the most effective strategy, but it is rarely applied. Without it, culling with repopulation and biosecurity are the two most efficient strategies, followed by vaccination. The low rank of vaccination comes from the fact that vaccination leads to asymptomatic diseases and increases the lifespan of infected poultry. At low levels, vaccination effectively

Table 11.3 List of control measures and their efficacies

Control measure	Affected parameters	Overall efficacy	Rank
Culling w/o repopulation	μ_d, ν_d	425.907	1
Culling with repopulation	μ_d,ν_d,Λ_d	212.453	3
Vaccination	β_d, ν_d, β	2.885	4
Biosecurity	β_d	212.454	2
Protective gear	β	1	5
Isolation	ν	0.999579	6

supports higher prevalence. One caveat that we should mention is that the actual control measures do not necessarily affect all parameters with 1% change. Pinpointing the exact change is not trivial.

11.3 Seasonality in Avian Influenza Modeling

It has been known for a long time that human influenza exhibits seasonality in the temperate zones. In more tropical climates, human flu shows more complex patterns. The reasons for the human flu seasonality remain unknown.

Avian influenza H5N1 affects many countries with different climates, and yet it exhibits seasonality similar to the human flu in temperate climates. This can be easily seen from the monthly human cases in Fig. 11.2.

Figure 11.2 shows that most of the cases occur in the period from December through March, and there are very few cases in the summer months. Moreover, in humans, seasonality can also be observed in H5N1 poultry outbreaks. To capture seasonality, we have to measure t in days or in months. Our preference will be to measure t in days.

11.3.1 An Avian Influenza Model with Seasonality

The cause of seasonality in H5N1 is completely unknown. Some authors have hypothesized that seasonality is intrinsic and should be modeled with autonomous models whose endemic equilibria can be destabilized and exhibit oscillations [107]. A more likely scenario is that seasonality is extrinsic. Perhaps the transmission rate β_d is not a constant, but a periodic function of t, or the survivability of H5N1 in the environment is periodic. A recent study considered a number of potential extrinsic mechanisms and their combinations as possible drivers of seasonality in H5N1 [157]. The study performed model selection on the resulting seven models and found out that Iwami's model with periodic transmission rate is the best fit to the cumulative number of human cases. We introduce that model here:

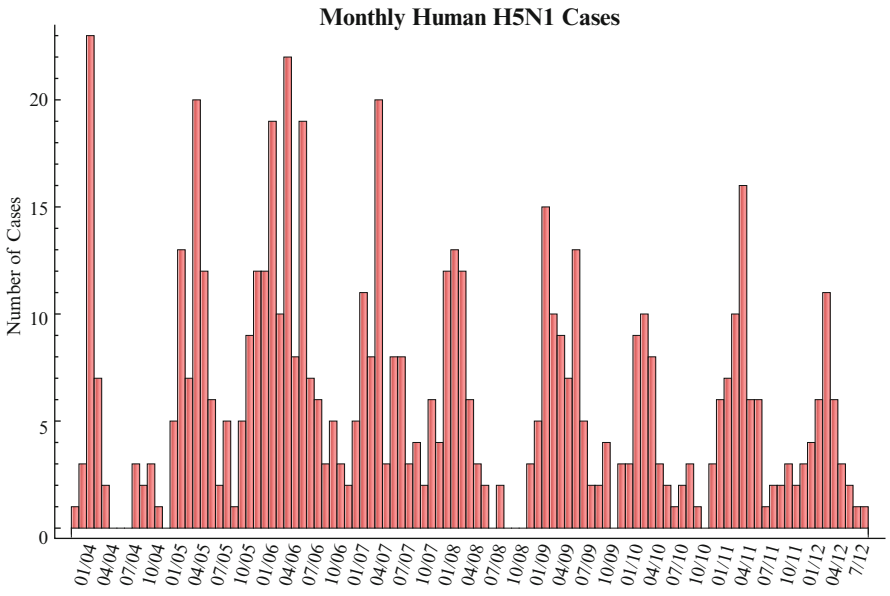

Fig. 11.2 Number of human cases of H5N1 by month. Data taken from [166]

$$\textbf{Domestic Birds:} \begin{cases} S_d'(t) = \Lambda_d - \beta_d(t) S_d I_d - \mu_d S_d, \\ I_d'(t) = \beta_d(t) S_d I_d - (\mu_d + \nu_d) I_d, \end{cases} \tag{11.4}$$

where the parameters have the same meanings as above. Seasonality is captured through a periodic transmission rate given by the periodic function

$$\beta_d(t) = \kappa_1 \sin\left(\frac{2\pi}{365}(t+\omega)\right) + \kappa_2. \tag{11.5}$$

Here κ_1 is the amplitude, ω is the horizontal shift, and κ_2 is the vertical shift. We want $\kappa_1 < \kappa_2$, so that $\beta_d(t) > 0$. The spillover model for humans takes the form

$$\textbf{Humans:} \begin{cases} S'(t) = \Lambda - \beta S I_d - \mu S, \\ I'(t) = \beta S I_d - (\mu + \nu) I. \end{cases} \tag{11.6}$$

Model (11.4)–(11.6) is well justified. As before, it can be fitted to the cumulative number of human cases of H5N1. We show the fit in Fig. 11.3, where we fitted the data through December 2009. These data are called calibration data. Then we extended the solution and plotted it alongside the incoming new data, called test data. It can be seen that the model describes well the incoming new data.

Model (11.4)–(11.6) is a model whose parameter β_d is an explicit function of the independent variable t. We have not considered models of this type before. Recall, however, that models in which one or more parameters are given functions of the independent variable are called *nonautonomous*.

An important class of nonautonomous models consists of those in which the parameters are periodic functions of the independent variable.

Definition 11.1. Models in which one or more parameters are periodic functions of the independent variable are called *periodic or seasonally forced* models.

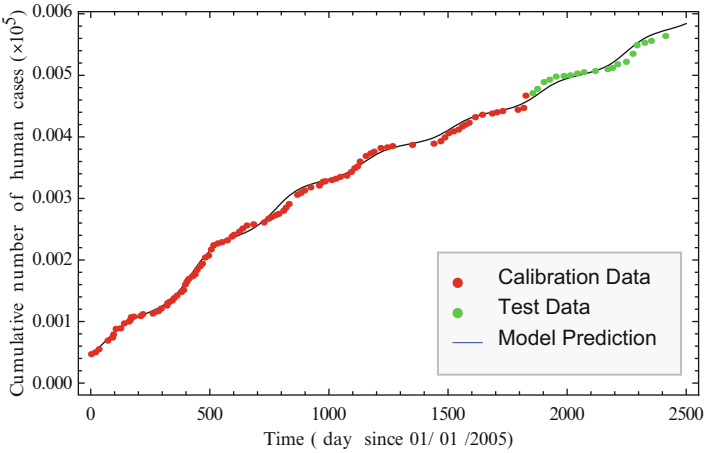

Fig. 11.3 Cumulative number of human cases of H5N1 in days

Methods for nonautonomous models include the Poincaré map and Floquet theory. We direct the reader to the many excellent books that cover this topic [155].

11.3.2 Tools For Nonautonomous Models

There are many tools that are designed to facilitate the study of nonautonomous periodic dynamical systems. Nonautonomous periodic dynamical systems are to a large extent analogous to autonomous dynamical systems. Here we explore two such tools.

11.3.2.1 The Poincaré Map

The Poincaré map was developed to study the intersection of the solution flow of a periodic orbit with the transversal cross section S. It is a tool for investigation of the n-dimensional dynamical system

$$x' = f(t,x). \tag{11.7}$$

The Poincaré map is defined as the point of return of the periodic orbit to S.

Suppose the flow ϕ generated by (11.7) is T-periodic, that is, $\phi(t+T,x_0)=\phi(t,x_0)$, and the cross section S of dimension $n-1$ is transversal to the vector field. Then the *Poincaré map* $\mathscr{P}(x): V \subset S \to S$ associates point x_0 in V with its point $\mathscr{P}(x_0)$ of the first return of the flow to S (see Fig. 11.4).

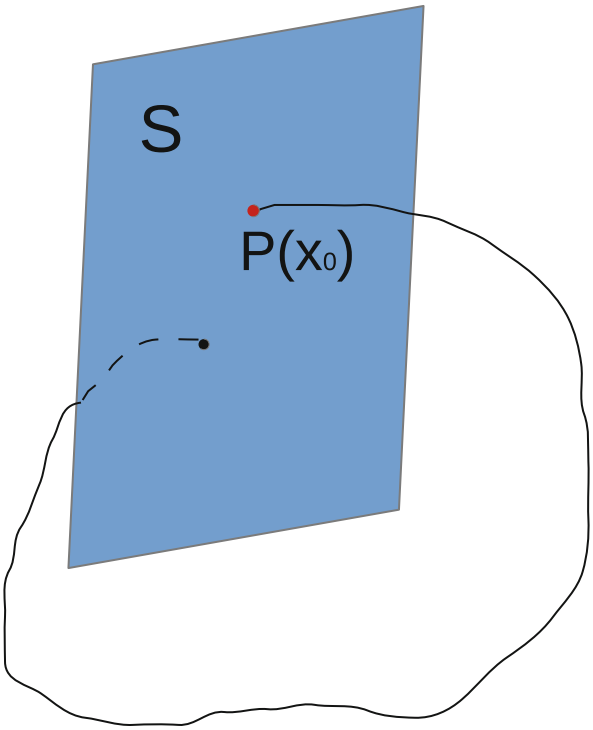

Fig. 11.4 A schematic description of the Poincaré map

The Poincaré map is relatively simple to study, but on the other hand, many of its properties are correlated to the properties of the flow. For instance, the stability of x of the map $\mathscr{P}(x)$ corresponds to the stability of the solution flow $\phi(t,x)$. If the solution flow has n (m) eigenvalues with negative (positive) real part, then the linearized map $D\mathscr{P}(x)$ has n (m) eigenvalues with modulus smaller (bigger) than one [155]. We utilize this property of the Poincaré map below.

11.3.2.2 Floquet Theory

Floquet theory provides another tool for investigating the local stability of solutions of periodic dynamical systems. Let

$$x' = A(t)x, \qquad x(0) = x_0, \tag{11.8}$$

be a linear nonautonomous periodic system, that is, $A(t+T) = A(t)$.

Definition 11.2. A matrix

$$\Phi(t) = [x^1(t), \ldots, x^n(t)],$$

where each column vector $x^j(t)$ is an independent solution of $x' = A(t)x$, is called a *fundamental matrix* of $x' = A(t)x$.

By definition,

$$\Phi'(t) = A(t)\Phi(t).$$

Theorem 11.1 (Floquet). *Each fundamental matrix of the T-periodic system $x' = A(t)x$ can be written as*

$$\Phi(t) = P(t)e^{Bt},$$

where $P(t)$ is T-periodic, $P(t+T) = P(t)$, and B is an $n \times n$ constant matrix.

The proof of this theorem can be found in [155] and is omitted. The following corollary shows the connection between a nonautonomous periodic linear system and the corresponding autonomous linear system.

Corollary 11.1. *The periodic system $x' = A(t)x$ is equivalent to the constant-coefficient system $y' = By$.*

Definition 11.3. The matrix $C = e^{BT}$ is called a *monodromy matrix*. The eigenvalues λ of the matrix B are called *Floquet exponents*. The eigenvalues $\rho = e^{\lambda T}$ of the matrix C are called *characteristic multipliers*.

11.3.2.3 Overview of Methods for Computing $\mathscr{R}_0$ in Periodic Models

When a nonautonomous system of differential equations is large, the analytical form of the reproduction number is difficult to compute. In this case, approximate methods must be used. Approximate methods compute an approximate value for the reproduction number. There are two types of approximate methods: analytical and computational. Among the analytical approximate methods is a method developed by Bacaër [19]. With this method, one calculates successive approximations of the reproduction number. Of course, analytically, one can compute perhaps two or three approximations, but these seem to be good enough. The advantage of the method is that one obtains an explicit formula for the approximate $\mathscr{R}_0$.

The reproduction number for periodic models has been more carefully defined in [164], in which the author proves its threshold properties and also gives an algorithm for its numerical computation. We notice that these results hold only when the coefficients of the nonautonomous model are periodic.

Another approach to computing the reproduction number is discussed in [45]. This approach is both approximate and exact for simpler models. The exact approach is very reminiscent of the approach we use below in this chapter for the computation of the reproduction number. Further discussion of the reproduction numbers including examples in which these computed reproduction numbers fail to provide a threshold for seasonally forced models can be found in [103].

11.3.3 Analyzing the Avian Influenza Model with Seasonality

Analyzing nonautonomous models is harder than analyzing autonomous models. For most of the nonautonomous models, even computing the reproduction number is a nontrivial task, and numerical methods must be used.

The model for domestic birds (11.4) can be separated from the full systems and investigated independently. The model is simple enough so that we can compute the reproduction number. The disease-free equilibrium of the model is time-independent and is given by $\mathscr{E}_0 = (\frac{\Lambda_d}{\mu_d}, 0)$. We linearize around the disease-free equilibrium. Let $x(t)$ be the perturbation of S_d, and $y(t)$ the perturbation in I_d. After dropping the quadratic terms and using the equations for the disease-free equilibrium to simplify, the system for the perturbations becomes

$$\begin{cases} x'(t) = -\beta_d(t)\dfrac{\Lambda_d}{\mu_d}y(t) - \mu_d x(t), \\ y'(t) = \beta_d(t)\dfrac{\Lambda_d}{\mu_d}y(t) - (\mu_d + \nu_d)y(t). \end{cases} \tag{11.9}$$

The second equation separates from the first. It is a linear equation with nonconstant coefficients. It can be solved explicitly. The solution is given by

$$y(t) = y(0)e^{\int_0^t \left(\beta_d(s)\frac{\Lambda_d}{\mu_d} - (\mu_d + \nu_d)\right) ds}. \tag{11.10}$$

To define the basic reproduction number, we first introduce the average of a periodic function over its period.

Definition 11.4. If $f(t)$ is a periodic function of period T, then the *average of* f is given by

$$< f >= \frac{1}{T}\int_0^T f(s)ds$$

Proposition 11.1. *If $f(t)$ is a periodic function of period T, then*

$$\lim_{t\to\infty}\frac{1}{t}\int_0^t f(s)ds = < f > .$$

Proof. Let $t \in [nT,(n+1)T)$. Then $t = nT+\varepsilon$, where $\varepsilon \in [0,T)$. Furthermore,

$$\int_0^t f(s)ds = \int_0^{nT} f(s)ds + \int_{nT}^{nT+\varepsilon} f(s)ds = n\int_0^T f(s)ds + \int_0^{\varepsilon} f(s)ds.$$

Dividing by $t = nT+\varepsilon$ and taking the limit $n\to\infty$, we have

$$\lim_{t\to\infty}\frac{1}{t}\int_0^t f(s)ds = \frac{1}{T}\int_0^T f(s)ds.$$

This completes the proof. □

Returning to Eq. (11.10), we see that

$$y(t) = y(0)e^{\left(\frac{1}{t}\int_0^t\left(\beta_d(s)\frac{\Lambda_d}{\mu_d}-(\mu_d+\nu_d)\right)ds\right)t} \approx y(0)e^{(<\beta_d>\frac{\Lambda_d}{\mu_d}-(\mu_d+\nu_d))t} \tag{11.11}$$

for t large enough. The expression on the right-hand side goes to $\pm\infty$ if and only if

$$<\beta_d>\frac{\Lambda_d}{\mu_d}-(\mu_d+\nu_d) > 0.$$

That prompts us to define the following reproduction number:

$$\mathscr{R}_0 = \frac{<\beta_d>\Lambda_d}{\mu_d(\mu_d+\nu_d)}. \tag{11.12}$$

We note that $\beta_d(t)$ is periodic with period 365 days. Hence $T = 365$. Clearly, we have the following traditional result:

Proposition 11.2. *If $\mathscr{R}_0 < 1$, then $y(t)\to 0$, and the disease-free equilibrium is locally asymptotically stable. If $\mathscr{R}_0 > 1$, then $|y(t)|\to\infty$, and the disease-free equilibrium is unstable.*

Furthermore, we can show that the disease-free equilibrium is globally stable. Indeed, we have the following result.

Proposition 11.3. *If $\mathscr{R}_0 < 1$, then $I_d(t)\to 0$ as $t\to\infty$.*

Proof. Adding the two equations, we have $N_d'(t) = \Lambda_d - \mu_d N_d - \nu_d I_d$, where $N_d = S_d + I_d$. This implies that $N_d'(t) \le \Lambda_d - \mu_d N_d$. We have shown before that in this case, $\limsup_t N_d(t) \le \frac{\Lambda_d}{\mu_d}$. Given $\varepsilon > 0$ such that

$$\mathscr{R}_0(\varepsilon) = \frac{< \beta_d > \left(\frac{\Lambda_d}{\mu_d} + \varepsilon\right)}{\mu_d + \nu_d} < 1,$$

there exists t_0 such that for every $t > t_0$, we have $N_d(t) < \frac{\Lambda_d}{\mu_d} + \varepsilon$. Since $\beta_d(t)$ is periodic, we can take $t_0 = nT$ and move the dynamical system so that $N_d(t) < \frac{\Lambda_d}{\mu_d} + \varepsilon$ is valid for all $t > 0$. Considering the equation for I_d, we have

$$I_d'(t) \leq [\beta(t)\left(\frac{\Lambda_d}{\mu_d} + \varepsilon\right) - (\mu_d + \nu_d)]I_d(t).$$

Solving this linear inequality, we have

$$I_d(t) \leq I_d(0)e^{\int_0^t [\beta(s)\left(\frac{\Lambda_d}{\mu_d} + \varepsilon\right) - (\mu_d + \nu_d)]ds}.$$

Thus, if $\mathscr{R}_0(\varepsilon) < 1$, we have $I_d(t) \to 0$ as $t \to \infty$. □

11.3.4 The Nonautonomous Avian Influenza Model with $\nu_d = 0$

The nonautonomous model (11.4) is very simple but capable of very complex behavior. To remove some of that complexity, in this subsection we analyze the model with $\nu_d = 0$. In this special case, the model can be reduced from a system of two equations to a single equation. In particular, we consider the system

$$\textbf{Domestic Birds:} \begin{cases} S_d'(t) = \Lambda_d - \beta_d(t)S_dI_d - \mu_dS_d, \\ I_d'(t) = \beta_d(t)S_dI_d - \mu_dI_d. \end{cases} \tag{11.13}$$

Adding the two equations, we obtain the equation of the total population size:

$$N_d'(t) = \Lambda_d - \mu_dN_d.$$

We know that the solution satisfies $N_d(t) \to \frac{\Lambda_d}{\mu_d}$. Let us assume for simplicity that $S_d(0) + I_d(0) = \frac{\Lambda_d}{\mu_d}$. Then $N_d(t) = \frac{\Lambda_d}{\mu_d}$ for all t. In this case,

$$S_d(t) = \frac{\Lambda_d}{\mu_d} - I_d(t).$$

From the second equation in (11.13) we obtain the following single equation in I_d:

$$I_d'(t) = \beta_d(t)(N_d - I_d(t))I_d(t) - \mu_dI_d(t), \tag{11.14}$$

where to simplify notation, we have set $N_d = \frac{\Lambda_d}{\mu_d}$. It can be shown as before that the reproduction number of this model is (see Problem 11.3)

$$\mathscr{R}_0 = \frac{< \beta_d > \Lambda_d}{\mu_d^2},$$

and the disease-free equilibrium is $\mathscr{E}_0 = (0)$. Equation (11.14) is a periodic Bernoulli equation [151] and has been studied before.

The main result for that equation is that it has a unique periodic solution $\xi(t)$ if $\mathscr{R}_0 > 1$. This periodic solution is globally asymptotically stable. We state these results in the following theorems:

Theorem 11.2. *Let $\beta_d(t)$ be periodic of period T. Assume also $\mathscr{R}_0 > 1$. Then equation (11.14) has a unique periodic solution $\xi(t)$.*

Proof. We consider Eq. (11.14) on the domain $\Omega = \{I_d : I_d \in [0, N_d]\}$. To show the existence of a periodic solution, we use the Poincaré map $\mathscr{P}$. The Poincaré map $\mathscr{P}$ maps the interval $[0, N_d]$ into itself. The Poincaré map is defined as follows. Let $I_d(0) = I_0$. Then

$$\mathscr{P}(I_0) = I_d(T, I_0),$$

where $I_d(t, I_0)$ is the solution of Eq. (11.14) that starts at I_0. In other words, $\mathscr{P}$ corresponds to the initial value I_0, the value of the solution at time $t = T$. Because of the properties of solutions to ODEs, the Poincaré map is one-to-one. Furthermore, it can be shown that it is continuously differentiable. It is not hard to show that $\mathscr{P}(0) = 0$ and $\mathscr{P}(N_d) < N_d$. The number $I_p \in [0, N_d]$ is an initial value of a periodic solution if and only if $\mathscr{P}(I_p) = I_p$, that is, if and only if I_p is a fixed point of the Poincaré map. Therefore, in order to show existence of a positive periodic solution of Eq. (11.14), we have to show that the Poincaré map has a fixed point. Define

$$v(t) = \frac{\partial I_d}{\partial I_0}(t, I_0).$$

Then the derivative of the Poincaré map is given as follows:

$$\mathscr{P}'(I_0) = \frac{\partial I_d}{\partial I_0}(T, I_0) = v(T).$$

To obtain the derivative of the Poincaré map, we differentiate equation (11.14) with respect to I_0. In this case, we obtain a differential equation in v:

$$v'(t) = v(t)[\beta_d(t)(N_d - I_d(t, I_0)) - \mu_d - \beta_d(t) I_d(t, I_0)]. \tag{11.15}$$

Differentiating the initial condition $I_d(0) = I_0$ with respect to I_0, we obtain that $v(0) = 1$. The differential equation for v can be solved, which gives the following expression for the derivative of the Poincaré map:

$$\mathscr{P}'(I_0) = e^{\int_0^T [\beta_d(t)(N_d - I_d(t, I_0)) - \mu_d - \beta_d(t) I_d(t, I_0)] dt}.$$

Clearly $\mathscr{P}'(I_0) > 0$, and hence the Poincaré map is increasing. Thus, if I_1 and I_2 are two initial conditions satisfying $I_1 < I_2$, then we have $\mathscr{P}(I_1) < \mathscr{P}(I_2)$. Furthermore,

$$\mathscr{P}'(0) = e^{T(<\beta_d> N_d - \mu_d)}.$$

Since $\mathscr{R}_0 > 1$, this means that the exponent is positive. Therefore, $\mathscr{P}'(0) > 1$. Hence for I_0 small enough,

$$\frac{\mathscr{P}(I_0) - \mathscr{P}(0)}{I_0} \approx \mathscr{P}'(0) > 1.$$

That implies that for I_0 small enough, $\mathscr{P}(I_0) > I_0$. Since, $\mathscr{P}(N_d) < N_d$, this means that the function $\mathscr{P}(I_0) - I_0$ changes sign in the interval $(0, N_d)$. Hence, there must exist I_p such that it becomes zero, that is, $\mathscr{P}(I_p) = I_p$.

To show uniqueness, we assume there are two distinct periodic solutions I_{p_1} and I_{p_2}. Without loss of generality, we may assume $I_{p_1} < I_{p_2}$. First, we note that if I_p is a periodic solution that satisfies model (11.14), then (see Problem 11.5)

$$\int_0^T [\beta_d(t)(N_d - I_d(t, I_p)) - \mu_d] dt = 0. \tag{11.16}$$

Second, for I_{p_1} and I_{p_2}, we have

$$|I_{p_1} - I_{p_2}| = |\mathscr{P}(I_{p_1}) - \mathscr{P}(I_{p_2})| = |\mathscr{P}'(I_m)||I_{p_1} - I_{p_2}|, \tag{11.17}$$

where I_m satisfies $I_{p_1} < I_m < I_{p_2}$. Furthermore, we have

$$\begin{aligned} \mathscr{P}'(I_m) =& e^{\int_0^T [\beta_d(t)(N_d - I_d(t, I_m)) - \mu_d - \beta_d(t) I(t, I_m)] dt} \\ &< e^{\int_0^T [\beta_d(t)(N_d - I_d(t, I_{p_1})) - \mu_d - \beta_d(t) I_d(t, I_m)] dt} \\ &< e^{-\int_0^T [\beta_d(t) I_d(t, I_m)] dt} < 1. \end{aligned} \tag{11.18}$$

Thus, we obtain a contradiction with (11.17). The contradiction is a result of the assumption that we have two distinct positive periodic solutions. □

Theorem 11.3. *Let $\beta_d(t)$ be periodic of period T. Assume also $\mathscr{R}_0 > 1$. Then the unique periodic solution $\xi(t)$ of Eq. (11.14) is globally stable, that is, if $I_d(t, I_0)$ is any solution starting from $I_d(0) = I_0$, then*

$$\lim_{t \to \infty} |I_d(t, I_0) - \xi(t)| = 0. \tag{11.19}$$

Proof. To complete the proof of the theorem, we have to establish the convergence to the periodic solution. We again assume $\mathscr{R}_0 > 1$, and we consider the solutions of Eq. (11.14). Let $I_d(t)$ be an arbitrary solution starting from the initial condition $I_d(0) = I_0$. We recall that I_p is the initial condition for the periodic solution. We assume that $I_p \neq I_0$. We have two choices, $\mathscr{P}(I_0) > I_0$ and $\mathscr{P}(I_0) < I_0$. We assume $\mathscr{P}(I_0) < I_0$. The other case can be addressed in a similar way. Since the Poincaré

map is increasing, we have $\mathscr{P}^n(I_0) < \mathscr{P}^{n-1}(I_0)$. Hence the sequence $\mathscr{P}^n(I_0)$ is a decreasing sequence. Since it is bounded from below, it must converge to a limit:

$$\lim_{n\to\infty} \mathscr{P}^n(I_0) = I_\infty.$$

It is not hard to see that the number I_∞ is a fixed point of the Poincaré map $\mathscr{P}(I_\infty) = I_\infty$. But the Poincaré map of model (11.14) has only two fixed points, $I_\infty = 0$ and $I_\infty = I_p$. Assume that $I_\infty = 0$. Then for some N, the number $\mathscr{P}^N(I_0)$ is small enough that from the properties of the Poincaré map, we have $\mathscr{P}^{N+1}(I_0) > \mathscr{P}^N(I_0)$, which contradicts the fact that the sequence is decreasing. Therefore, $I_\infty = I_p$. Consequently, the limit (11.19) holds. This completes the proof of the theorem. □

11.3.5 The Full Nonautonomous Avian Influenza Model

The nonautonomous model with $\nu_d \neq 0$ is a two-dimensional system and cannot be reduced to a single equation. Unlike autonomous two-dimensional models, which can exhibit only oscillations, two-dimensional nonautonomous models are capable of exhibiting chaotic behavior. This is the case with model (11.4). For small ν_d, the unique oscillatory solution is still stable, but as ν_d increases, period-doubling occurs, and the solution transitions to a chaotic solution. This can be seen in the bifurcation diagram in Fig. 11.5.

The chaotic solution exhibits the pattern typical for H5N1 outbreak. We show this in Fig. 11.6

Acknowledgements The author thanks Necibe Tuncer for help with fittings.

Appendix

In this appendix, we include Matlab code that fits model (11.1)–(11.2) to the data in Table 11.1.

```
function Ch11fitting_model1

clear all
close all
clc

load AFluDatCumHalf14.txt %Imports the data file

tdata =  AFluDatCumHalf14(:,1);
qdata =  AFluDatCumHalf14(:,2);

```

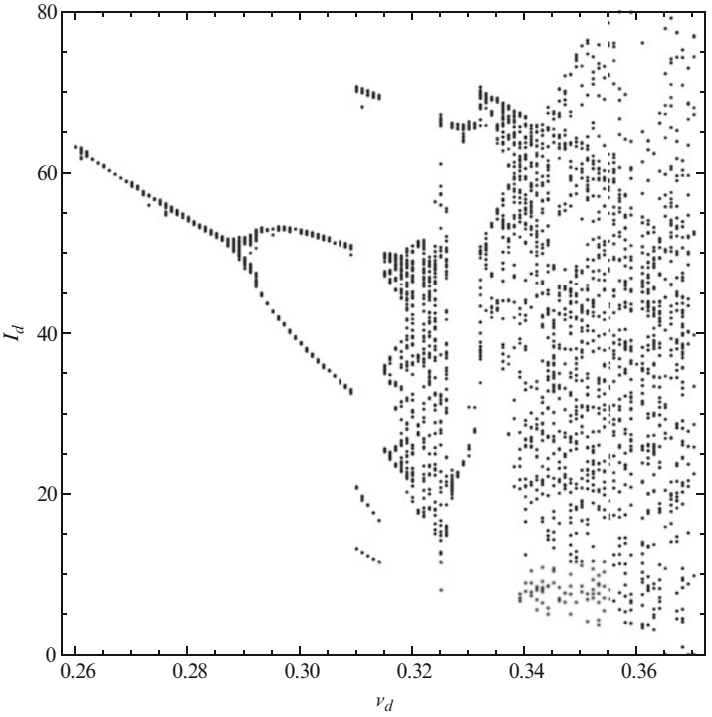

Fig. 11.5 Period-doubling and transition to chaos as ν_d increases. Parameters for the Figure are $\Lambda_D = 1020$, $\mu_d = 1/(2*356)$, $\kappa_1 = 0.00005111486$, $\kappa_2 = 0.00032621758$, $\omega = 127$

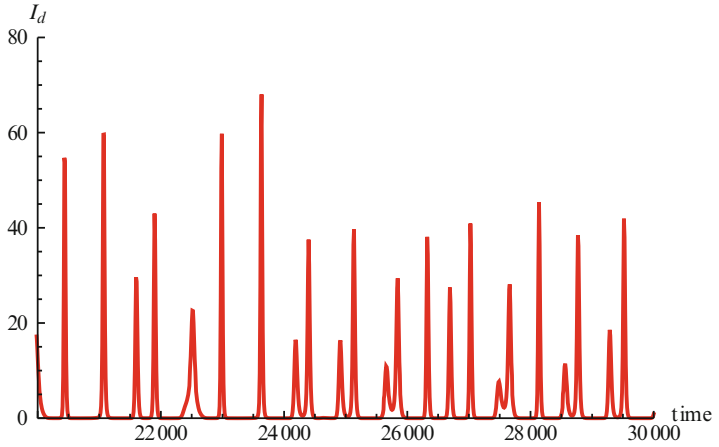

Fig. 11.6 Chaotic solution exhibits outbreak pattern. Parameters as in Fig. 11.5. In addition, $\nu_d = 0.35$

```
tforward = (0:0.01:9)';
tmeasure = [1:50:901]';

format long

    function dy = model_1(t,y,k)

    Lb = 1200;
    L  = 1000;
    mb = 1/2;
    nb = 36.5;
    mu = 1/65;
    nu = 36.5;

    dy = zeros(5,1);

    dy(1) = Lb -k(1)*y(1)*y(2)-mb*y(1);
    dy(2) = k(1)*y(1)*y(2)-(nb+mb)*y(2);
    dy(3) = L - k(2)*y(3)*y(2)-mu*y(3);
    dy(4) = k(2)*y(3)*y(2)-(mu+nu)*y(4);
    dy(5) = k(2)*y(3)*y(2);

    end

    function q = model1(k,tdata)

    [T,Y] = ode23s(@(t,y)(model_1(t,y,k)),tforward,
                           [2400  k(3)  65000  0.0007  ...
                               .0007]);

    q = Y(tmeasure(:),5);

    end

k = [0.0158  0.00000001063 0.9]; % Initial values for ...
    parameters

lb = [0.0           0.0              0.0];



for i = 1:5

  [k,resnorm] = lsqcurvefit(@model1,k,tdata,qdata,lb,[],...
   optimset('Disp','iter','TolX',10^(-20),'TolFun',10^(-20)))
 end


 [T,Y] = ode15s(@(t,y)(model_1(t,y,k)),tforward,[2400 ...
        k(3)  65000  .0007  .0007]);



figure(1)
```

```
64
65    plot(tdata,qdata,'r.');
66    hold on
67    plot(tforward,Y(:,5),'b-');
68
69
70  end
71
72  end
```

Problems

11.1. For model (11.1)–(11.2), obtain a list of the countries that have human cases from the main source of data [166]. Use [58] to obtain the number of poultry units for these countries. Use [167] to determine the human population of the affected countries. Parameterize model (11.1)–(11.2) with these data.

11.2. Consider the AI model with pandemic strain [80]

$$\textbf{Domestic Birds:} \begin{cases} S_d'(t) = \Lambda_d - \beta_d S_d I_d - \mu_d S_d, \\ I_d'(t) = \beta_b S_d I_d - (\mu_d + \nu_d) I_d. \end{cases} \tag{11.20}$$

The spillover model for humans with pandemic strain takes the form

$$\textbf{Humans:} \begin{cases} S'(t) = \Lambda - \beta S I_d - \beta_Z S Z - \mu S, \\ I'(t) = \beta S I_d - (\mu + \nu + \rho) I, \\ Z'(t) = \rho I + \beta_Z S Z - (\mu + \nu_Z) Z. \end{cases} \tag{11.21}$$

where Z is the number of individuals infected by the pandemic strain.

(a) Compute the reproduction numbers of the avian and the pandemic strains.
(b) Fit the model to the data in Table 11.1. Take $\nu_z = 36.5$. Estimate the reproduction numbers from the fit. The reproduction number of the pandemic strain should be between 1.5 and 3.
(c) Compute the invasion number of the pandemic strain.
(d) Compute the elasticity of the pandemic invasion number with respect to I_d^*. Culling facilitates invasion, but how pronounced is that effect?

11.3. Consider the reproduction number

$$\mathscr{R}_0 = \frac{< \beta_d > \Lambda_d}{\mu_d^2}.$$

Using the periodicity properties of sin, simplify it as much as possible.

11.4. Show that model (11.14) has as a reproduction number

$$\mathscr{R}_0 = \frac{< \beta_d > \Lambda_d}{\mu_d^2}.$$

11.5. Prove equality (11.16).

11.6. Let $\beta(t)$, $\mu(t)$, and $\gamma(t)$ be periodic with period T. Consider the model

$$I'(t) = \beta(t)(1-I(t))I(t) - (\mu(t)+\gamma(t))I(t).$$

(a) Compute the reproduction number of this model.
(b) Show that $\mathscr{R}_0$ computed in (a) gives a threshold, that is, the DFE is locally asymptotically stable if $\mathscr{R}_0 < 1$ and unstable if $\mathscr{R}_0 > 1$.
(c) Sow that the DFE is globally asymptotically stable if $\mathscr{R}_0 < 1$.

11.7. Let $\beta(t)$, $\mu(t)$, and $\gamma(t)$ be periodic with period T. Consider the model (see Problem 11.6)

$$I'(t) = \beta(t)(1-I(t))I(t) - (\mu(t)+\gamma(t))I(t).$$

(a) Show that the model has a unique periodic solution if $\mathscr{R}_0 > 1$.
(b) Show that the periodic solution is globally asymptotically stable.

11.8. Let $\beta(t)$, $\mu(t)$, and $\gamma(t)$ be periodic with period T. Consider the two-strain model

$$\begin{aligned} I_1'(t) &= \beta_1(t)(1-I_1(t)-I_2(t))I_1(t) - (\mu_1(t)+\gamma_1(t))I_1(t), \\ I_2'(t) &= \beta_2(t)(1-I_1(t)-I_2(t))I_2(t) - (\mu_2(t)+\gamma_2(t))I_2(t). \end{aligned} \tag{11.22}$$

(a) Define the reproduction number of each strain.
(b) Let $\xi_1(t)$ and $\xi_2(t)$ be the periodic solutions of strain one alone and strain two alone. Define the invasion numbers of strain one and strain two.

Hint: You have to look at the stability of the solution $(\xi_1(t),0)$. Define the Floquet exponent for strain two and read off the invasion number.